
Article:
Ishak, D., Zhu, Z.Q. and Howe, D. (2005) Eddy-current loss in the rotor magnets of permanent-magnet brushless machines having a fractional number of slots per pole. IEEE Transactions on Magnetics, 41 (9). pp. 2462-2469. ISSN 0018-9464

https://doi.org/10.1109/TMAG.2005.854337

Eddy-Current Loss in the Rotor Magnets of Permanent-Magnet Brushless Machines Having a Fractional Number of Slots Per Pole

Dahaman Ishak, Z. Q. Zhu, *Senior Member, IEEE*, and David Howe

Department of Electronic and Electrical Engineering, University of Sheffield, Sheffield S1 3JD, U.K.

We develop an analytical model for predicting the eddy-current loss in the rotor magnets of permanent-magnet brushless machines that have a fractional number of slots per pole, when either all the teeth or only alternate teeth are wound, and in which the unwound teeth may be narrower than the wound teeth. The model enables the magnetic field distribution in the air gap and magnet regions to be determined, by neglecting the eddy-current redistribution effect and assuming that the eddy currents are resistance limited. It can account for space-harmonic magnetomotive forces (MMFs) resulting from the winding distribution and time-harmonic MMFs due to nonsinusoidal phase currents, as well as for the effect of curvature and circumferential segmentation of the magnets. We have validated the model by finite-element analysis, and used it to investigate the eddy-current loss in the magnets of three surface-mounted magnet brushless motors that have similar slot and pole numbers, and employ identical rotors but different stators, when they are operated in brushless ac (BLAC) and dc (BLDC) modes. We show that the stator winding configuration, as well as the operational mode, significantly influence the resultant eddy-current loss.

Index Terms—**Brushless machines, eddy currents, fractional slots/per pole, permanent magnet.**

I. Introduction

THE eddy-current loss that is induced in the permanent magnets of brushless machines is often neglected [1]. However, this assumption may not always be justified. For example, machine designs are emerging in which the torque is produced by the interaction of a space-harmonic magnetomotive force (MMF) with the permanent magnets and which employ concentrated windings. Although this results in short end-windings, and, hence, a low copper loss, and a high power density [2]–[7], and the coils may be wound only on alternate teeth so as to enhance fault-tolerance [5]–[7], eddy currents will be induced in the magnets by forward and backward rotating MMFs. The situation may be aggravated further by time harmonics in the phase currents. Due to the relatively high electrical conductivity of rare-earth magnets, the resultant eddy-current loss can be significant, and may cause a substantial temperature rise and result in partial irreversible demagnetization of the magnets, especially in machines with a high electric loading, a high rotational speed, or a high pole number. A comprehensive literature review on rotor eddy-current losses was presented in [8].

This paper extends the model that was presented in [7] by considering time harmonics in the stator MMF distribution, and proposes a simplified analytical model, with reference to [8]–[11], which assumes that the eddy currents are only induced in the permanent magnets and are resistance limited. The model is formulated in two-dimensional (2-D) polar coordinates, and represents the stator ampere-conductor distribution by an equivalent current sheet distributed over the stator slot openings. Thus, Laplace's equation, which governs the vector magnetic potential in the air-gap and magnet regions, can be solved using the separation of variables method. Subsequently, an expression for the eddy-current loss in the magnets can be derived, accounting for space-harmonic and time-harmonic MMFs, as well as the effect of curvature and circumferential segmentation of the magnets. The following assumptions are made in the derivation.

- The machines are three-phase, although the analysis is readily applicable to higher phase number machines.
- The winding currents are approximated by an equivalent current sheet of infinitesimal thickness distributed over the stator slot openings.
- The stator and rotor iron cores are infinitely permeable and have zero electrical conductivity.
- The induced eddy currents are axially-directed only, i.e., end-effects are neglected.
- The magnets have a relative recoil permeability of $\mu_m = 1$, which simplifies the analysis but does not unduly compromise the accuracy of the predictions, as will be shown later.
- The magnets have an electrical conductivity of σ_m.
- The modifying effect of the induced eddy currents on the applied magnetic field is neglected.
- The air-gap permeance variation due to stator slotting is neglected.

The developed analytical model is employed to investigate the eddy-current loss in the magnets of three 12-slot/10-pole surface-mounted magnet motors, in two of which all the teeth have the same width, one having all the teeth wound and the other only having coils on alternate teeth. The third motor also has coils on alternate teeth, the width of which is increased in order to maximize the torque density. Further, since the slot number N_s and pole number $2p_r$ are related by $2p_r = N_s \pm 2$, viz. 10 poles and 12 slots, the electromagnetic torque is produced by the interaction of the fifth space-harmonic MMF with the

Digital Object Identifier 10.1109/TMAG.2005.854337

TABLE I
PARAMETERS OF THREE-PHASE, 5.5-Nm PERMANENT-MAGNET BRUSHLESS MOTORS

Parameter	
Pole number, $2p$	10
Slot number, N_s	12
Stack length, l_a	50 mm
Airgap length, g	1 mm
Slot opening, b_o	2 mm
Stator bore radius, R_s	28.5 mm
Magnet outer radius, R_m	27.5 mm
Magnet inner radius, R_r	24.5 mm
Magnet thickness, h_m	3 mm
Magnet remanence, B_r	1.2 T
Magnet conductivity, σ_m	6.67 x 10^5 $(\Omega m)^{-1}$
Series turns per phase, N_{ph}	132
Tooth tip width in Motors I and II	12.92mm
Tooth tip width in Motor III	16.91mm on wide teeth 8.95mm on narrow teeth
Pole-pitch	17.91mm

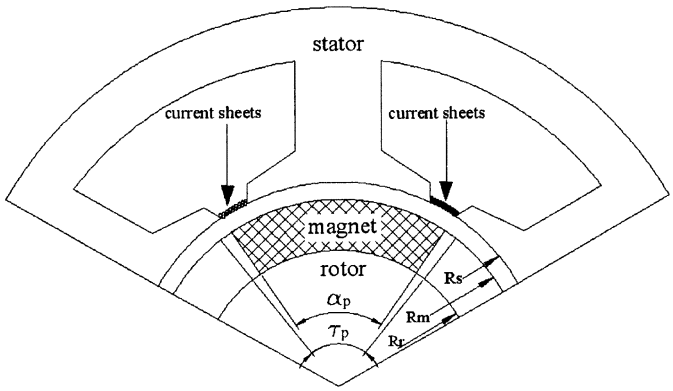

Fig. 1. Equivalent current sheet distribution.

rotor magnets. The analytically predicted eddy-current loss in the magnets is validated by finite-element analyses (FEA) under both brushless ac (BLAC) and dc (BLDC) modes of operation. Table I shows the motor parameters.

II. EQUIVALENT CURRENT SHEETS

In order to predict the time-varying armature reaction field in the air-gap and magnet regions, the stator ampere-conductor distribution is represented by an equivalent current sheet of infinitesimal thickness disposed over the slot openings, as illustrated in Fig. 1. In the motor in which all the teeth are wound, each slot accommodates conductors of two different coils, whereas in the motors in which only alternate teeth are wound each slot accommodates conductors of a single coil, albeit the number of coils per phase being halved and the number of turns per coil doubled in order to achieve a similar phase back-electromotive force constant. Fig. 2 shows the cross section and winding arrangement for each of the three motors [4]. Fourier series expressions for the equivalent current sheets, assuming balanced three-phase windings, are

$$J_s(\alpha, R_s, t) = \sum_u^\infty \sum_v^\infty J_{uv} \sin[up_r\omega_r t \pm v\alpha \pm \alpha_0 + \theta_u] \quad (1)$$

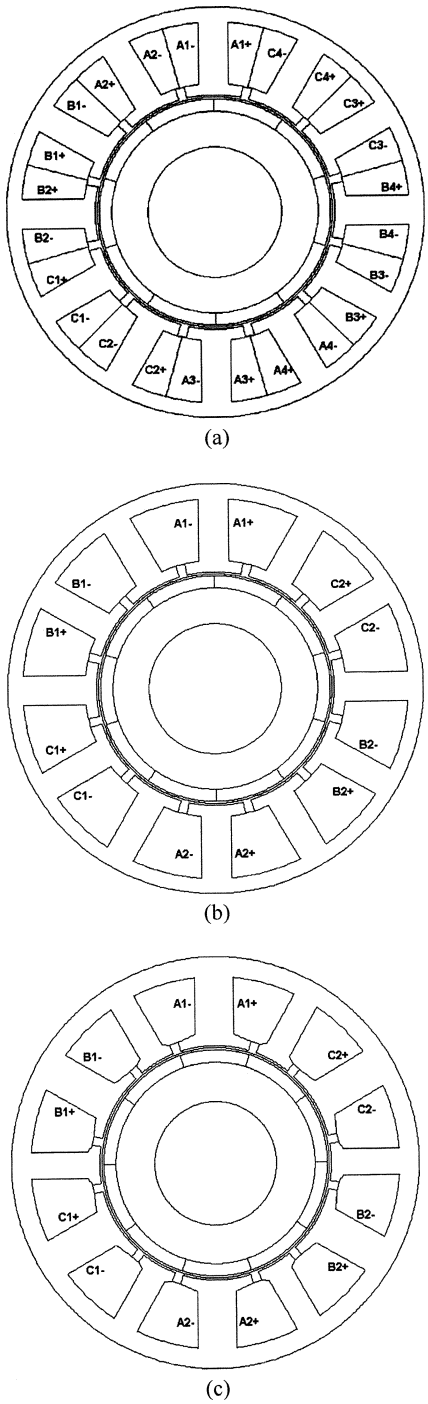

Fig. 2. Winding distributions for the 12-slot/10-pole motors. (a) Motor I—all teeth wound. (b) Motor II—alternate teeth wound. (c) Motor III—alternate teeth wound on wider teeth.

for the motor in which all the teeth are wound, and

$$J_s(\alpha, R_s, t) = \mp \sum_u^\infty \sum_v^\infty J_{uv} \cos[up_r\omega_r t \pm v\alpha + \theta_u] \quad (2)$$

for the motors in which only alternate teeth are wound, where

$$J_{uv} = \frac{3N_{\rm ph}I_u}{\pi R_s} K_{\rm sov} K_{wv} \quad \text{and} \quad v = 3c \pm u, \quad c = 0, \pm 1, \pm 2, \ldots \quad (3)$$

u is the time-harmonic order in the phase current waveform, v is the space-harmonic MMF order, α is the rotor position in mech. rads, α_o is $v\pi/N_s$, R_s is the stator bore radius, I_u is the amplitude of the harmonic phase current, p_r is the number of rotor magnet pole-pairs, $N_{\rm ph}$ is the total number of series turns per phase, ω_r is the rotor speed, θ_u is the phase current harmonic angle, $K_{\rm sov}$ is the slot opening factor and $K_{wv} = K_{pv}K_{dv}$ is the winding factor, K_{pv} and K_{dv} being the winding pitch factor and the winding distribution factor, respectively, where

$$K_{wv} = \sin^2\left(v\frac{p_r\pi}{N_s}\right) \text{ when all the teeth are wound,} \quad \text{Motor I} \quad (4)$$

$$K_{wv} = \sin\left(v\frac{p_r\pi}{N_s}\right) \text{ when only alternate teeth are wound,} \quad \text{Motor II} \quad (5)$$

$$K_{wv} = 1 \text{ when alternate teeth are wound on wider teeth,} \quad \text{Motor III.} \quad (6)$$

III. Armature Reaction Field

In terms of the vector magnetic potential $\boldsymbol{A}$, Laplace's equation, which governs the armature reaction field in the air-gap and magnet regions, neglecting the eddy-current redistribution effect in the magnets, is

$$\nabla^2 A = 0 \quad (7)$$

for which the general solution is

$$A(r,\alpha) = \sum_v^{\infty}(C_v r^{vp_s} + D_v r^{-vp_s})\cos(vp_s\alpha) \quad (8)$$

where p_s is the number of pole-pairs in the stator winding MMF. The magnetic field components are related to $\boldsymbol{A}$ by

$$B_r = \frac{1}{r}\frac{\partial A}{\partial \alpha} \quad \text{and} \quad B_\theta = -\frac{\partial A}{\partial r} \quad (9)$$

and the boundary conditions are given by

$$B_\theta|_{r=R_r} = 0 \quad \text{and} \quad H_\theta|_{r=R_s} = J_s \quad (10)$$

where R_r is the inner radius of the magnets. Analytical expressions for the vector magnetic potential can be derived as

$$A(r,\alpha,t) = \mu_o \sum_u^{\infty}\sum_v^{\infty} \frac{J_{uv}R_s^{-vp_s+1}}{G_v(vp_s)}\left(r^{vp_s} + R_r^{2vp_s}r^{-vp_s}\right) \times \sin(up_r\omega_r t \pm vp_s\alpha \pm \alpha_o + \theta_u) \quad (11)$$

for a motor in which all the teeth are wound, and

$$A(r,\alpha,t) = \mp\mu_o \sum_u^{\infty}\sum_v^{\infty} \frac{J_{uv}R_s^{-vp_s+1}}{G_v(vp_s)}\left(r^{vp_s} + R_r^{2vp_s}r^{-vp_s}\right) \times \cos(up_r\omega_r t \pm vp_s\alpha + \theta_u) \quad (12)$$

for a motor in which only alternate teeth are wound, where G_v is given by

$$G_v = 1 - \left(\frac{R_r}{R_s}\right)^{2vp_s}. \quad (13)$$

Therefore, the radial and tangential components of the armature reaction field are

$$B_r(r,\alpha,t) = \pm\mu_o \sum_u\sum_v \frac{J_{uv}R_s^{-vp_s+1}}{G_v}\left(r^{vp_s-1} + R_r^{2vp_s}r^{-vp_s-1}\right) \times \cos(up_r\omega_r t \pm vp_s\alpha \pm \alpha_o + \theta_u) \quad (14)$$

$$B_\theta(r,\alpha,t) = -\mu_o \sum_u\sum_v \frac{J_{uv}R_s^{-vp_s+1}}{G_v}\left(r^{vp_s-1} - R_r^{2vp_s}r^{-vp_s-1}\right) \times \sin(up_r\omega_r t \pm vp_s\alpha \pm \alpha_o + \theta_u) \quad (15)$$

for a motor in which all the teeth are wound, and

$$B_r(r,\alpha,t) = \mu_o \sum_u\sum_v \frac{J_{uv}R_s^{-vp_s+1}}{G_v}\left(r^{vp_s-1} + R_r^{2vp_s}r^{-vp_s-1}\right) \times \sin(up_r\omega_r t \pm vp_s\alpha + \theta_u) \quad (16)$$

$$B_\theta(r,\alpha,t) = \pm\mu_o \sum_u\sum_v \frac{J_{uv}R_s^{-vp_s+1}}{G_v}\left(r^{vp_s-1} - R_r^{2vp_s}r^{-vp_s-1}\right) \times \cos(up_r\omega_r t \pm vp_s\alpha + \theta_u) \quad (17)$$

for a motor in which only alternate teeth are wound.

If the phase current waveforms in the three-phase windings are assumed to be sinusoidal or rectangular, and to have a peak value of 10 A, Figs. 3(a) and 4(a), respectively, show instantaneous field distributions when $\rm i_a = 10$ A and $\rm i_b = i_c = -5$ A, corresponding to BLAC operation, and $\rm i_a = 0$ A, $\rm i_b = -10$ A, and $\rm i_c = 10$ A, corresponding to BLDC operation. Analytically predicted air-gap flux density distributions at the surface of the magnets are compared with those obtained from FEA in Figs. 3(b)–(g) and 4(b)–(g). Since the motors in which only alternate teeth are wound have twice the number of turns per coil the maximum radial component of air-gap flux density is approximately twice that of the motor in which all the teeth are wound. As can be seen, in both modes of operation, the analytically predicted flux density distributions are in good agreement with those obtained from FEA. However, close inspection of Figs. 3 and 4 reveals that the analytically predicted flux density is slightly higher than that calculated by FEA since the permeance variation due to the stator slots is neglected in the analytical model. This is justified since the permeance harmonics due to the stator slots decay rapidly with distance from the stator bore [12], and, in general, the representation of the stator MMF distribution by an equivalent current sheet without accounting for the stator slot openings is sufficiently accurate. However, if the

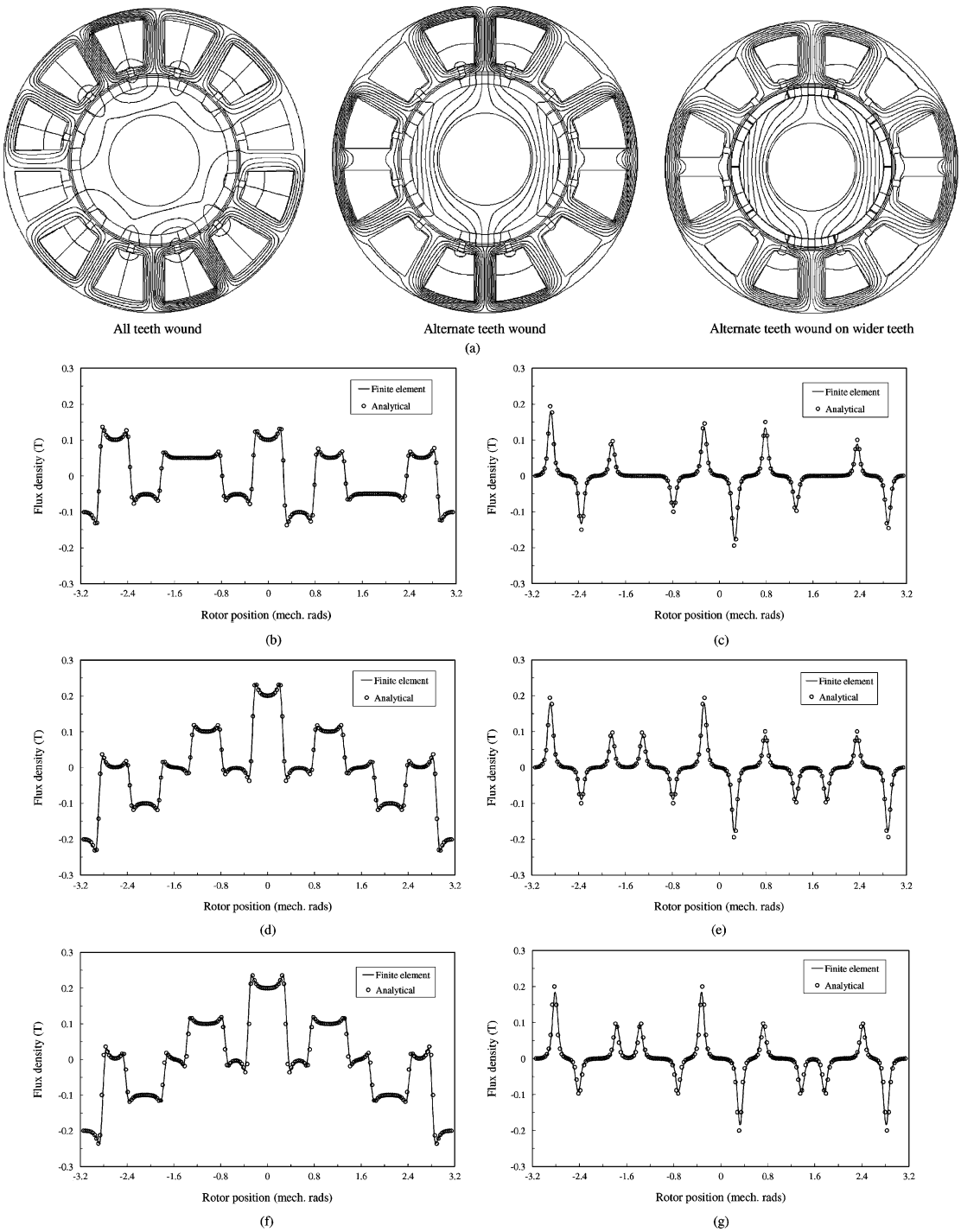

Fig. 3. Instantaneous armature reaction field and air-gap flux density distributions, for BLAC mode ($i_a = 10$ A, and $i_b = i_c = -5$ A). (a) Field distributions. (b) Radial flux density component—all teeth wound. (c) Circumferential flux density component—all teeth wound. (d) Radial flux density component—alternate teeth wound. (e) Circumferential flux density component—alternate teeth wound. (f) Radial flux density component—alternate teeth wound on wider teeth. (g) Circumferential flux density component—alternate teeth wound on wider teeth.

width of the slot openings is considered to be large, the influence of slotting may be accounted for by introducing a "2-D" permeance function in the analytical field [12] and eddy-current loss [11] calculation. However, it then becomes much more complicated.

It is also worth noting that, since it has been assumed that $\mu_m = 1$ in both the analytical and finite-element calculations, the armature reaction field for the actual motors, for which $\mu_m = 1.05$, will be slightly underestimated. However, the error will be significantly less than 5% since the effective permeance is due to the air gap as well as the magnets.

IV. Eddy-Current Loss

Since rare-earth magnets have a relatively low electrical resistivity and recoil permeability, for most practical machines, the

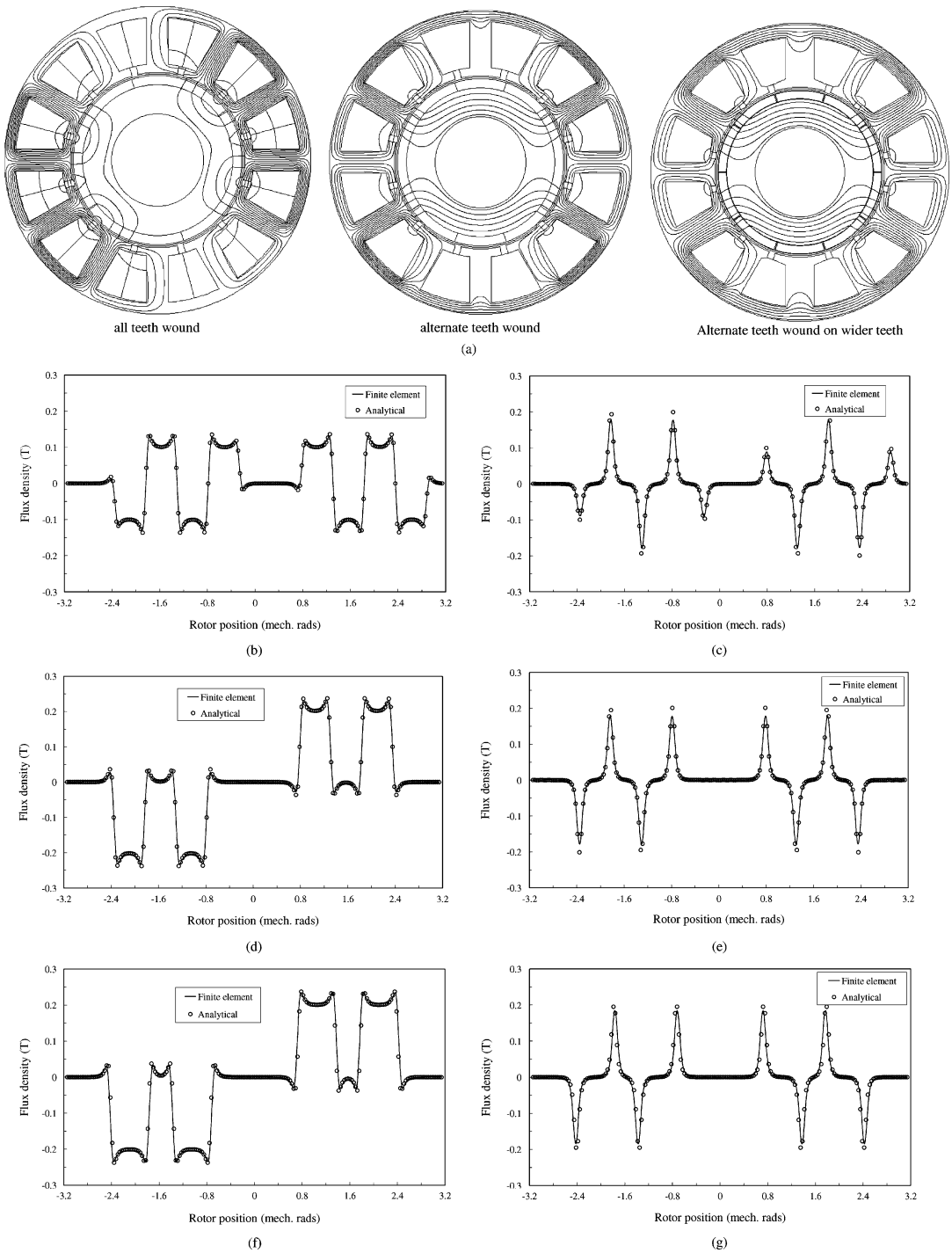

Fig. 4. Instantaneous armature reaction field distributions and air-gap flux density distributions, for BLDC mode ($i_a = 0$ A, $i_b = -10$ A, and $i_c = 10$ A). (a) Field distribution. (b) Radial flux density component—all teeth wound. (c) Circumferential flux density component—all teeth wound. (d) Radial flux density component—alternate teeth wound. (e) Circumferential flux density component—alternate teeth wound. (f) Radial flux density component—alternate teeth wound on wider teeth. (g) Circumferential flux density component—alternate teeth wound on wider teeth.

skin depth at the inducing frequencies is significantly greater than both the magnet pole-arc and radial thickness. Hence, the induced eddy currents are usually resistance limited, and the associated loss in the magnets can be derived directly from the armature reaction field. For example, for the motors under consideration, at the fundamental time harmonic, the skin depth is 104 mm at 400 rpm, and this reduces to 52 mm at 1600 rpm, whereas the magnet pole-arc and thickness are $\sim$ 17 and 3 mm, respectively. Even for low-order time harmonics, such as $u = 5$ and 7, which are significant in the rectangular phase current waveform under BLDC operation, it is still reasonable to assume that the skin depth is greater than both the magnet pole-arc and thickness, as will be evident later.

In order to determine the induced eddy currents, the expressions for the equivalent current sheets and the vector magnetic potential have to be transformed from the stationary reference

frame α to the rotating reference frame such that $\alpha = \theta_r + \omega_r t$. Hence

$$J_s(\theta_r, R_s, t) = \sum_u^\infty \sum_v^\infty J_{uv} \sin[(up_r \pm vp_s)\omega_r t \pm vp_s\theta_r \pm \alpha_0 + \theta_u] \tag{18}$$

$$A(r, \theta_r, t) = \mu_o \sum_u^\infty \sum_v^\infty \frac{J_{uv} R_s^{-vp_s+1}}{G_v(vp_s)} \left(r^{vp_s} + R_r^{2vp_s} r^{-vp_s}\right) \times \sin[(up_r \pm vp_s)\omega_r t \pm vp_s\theta_r \pm \alpha_o + \theta_u] \tag{19}$$

for motors in which all the teeth are wound, and

$$J_s(\theta_r, R_s, t) = \mp \sum_u^\infty \sum_v^\infty J_{uv} \cos[(up_r \pm vp_s)\omega_r t \pm vp_s\theta_r + \theta_u] \tag{20}$$

$$A(r, \theta_r, t) = \mp\mu_o \sum_u^\infty \sum_v^\infty \frac{J_{uv} R_s^{-vp_s+1}}{G_v(vp_s)} \left(r^{vp_s} + R_r^{2vp_s} r^{-vp_s}\right) \times \cos[(up_r \pm vp_s)\omega_r t \pm vp_s\theta_r + \theta_u] \tag{21}$$

for motors in which only alternate teeth are wound.

The induced eddy currents in the magnets due to the time-varying armature reaction field can then be calculated from

$$J_m(r, \theta_r, t) = -\frac{1}{\rho}\frac{\partial A(r, \theta_r, t)}{\partial t} + C(t) \tag{22}$$

where ρ is the electrical resistivity of the magnets and C is an integration constant which forces the net total current flowing in each magnet segment to be zero at any instant, i.e.,

$$\int_{R_r}^{R_m} \int_{-\frac{\alpha_p}{2}}^{\frac{\alpha_p}{2}} J_m r dr d\theta_r = 0 \tag{23}$$

where R_m and α_p are the magnet outer radius and pole-arc, respectively. Therefore, the eddy-current loss per unit axial length in each magnet, irrespective of whether all the teeth or only alternate teeth are wound, is given by

$$P = 2p_r \frac{\omega_r}{2\pi} \int_0^{\frac{2\pi}{\omega_r}} \int_{R_r}^{R_m} \int_{-\frac{\alpha_p}{2}}^{\frac{\alpha_p}{2}} \rho J_m^2 r \, dr \, d\theta \, dt = \sum_u \sum_v (P_{cuv} + P_{auv}) \tag{24}$$

where the variables P_{cuv} and P_{auv} are given by

$$P_{cuv} = \frac{\mu_o^2 \alpha_p}{\rho} p_r \sum_u^\infty \sum_v^\infty \frac{J_{uv}^2 (up_r \pm vp_s)^2 \omega_r^2}{G_v^2 (vp_s)^2} \times \left\{ \left(\frac{R_m}{R_s}\right)^{2vp_s} \frac{R_s^2 R_m^2}{(2vp_s+2)} \left[1 - \left(\frac{R_r}{R_m}\right)^{2vp_s+2}\right] + \left(\frac{R_r}{R_s}\right)^{2vp_s} R_s^2 (R_m^2 - R_r^2) + \left(\frac{R_r}{R_s}\right)^{2vp_s} R_s^2 R_r^2 F_v \right\} \tag{25}$$

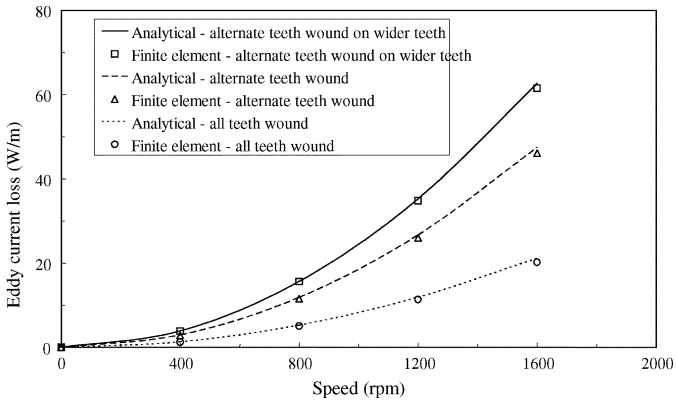

Fig. 5. Variation of eddy-current loss with rotor speed at rated current, BLAC mode.

TABLE II
ALL TEETH WOUND—EDDY-CURRENT LOSS, BLAC MODE

Space harmonic ν	Loss in all magnets (W/m)			
	400rpm	800rpm	1200rpm	1600rpm
1	0.18	0.43	0.98	1.735
5	0	0	0	0
7	1.15	4.60	10.35	18.4
11	0.001	0.005	0.011	0.02
13	0.001	0.002	0.005	0.008
17	0.010	0.04	0.091	0.16
19	0.047	0.19	0.42	0.75
Total	1.32	5.27	11.85	21.07

$$F_v = \begin{cases} \frac{\left(\frac{R_m}{R_r}\right)^{-2vp_s+2} - 1}{(-2vp_s+2)} & \text{for } vp_s \neq 1 \\ \ln\left(\frac{R_m}{R_r}\right) & \text{for } vp_s = 1 \end{cases} \tag{26}$$

$$P_{auv} = \left[-\frac{8\mu_o^2}{\alpha_p \rho} p_r \sum_u^\infty \sum_v^\infty \frac{J_{uv}^2 H_v^2}{G_v^2 (vp_s)^4} \times \frac{(up_r \pm vp_s)^2 \omega_r^2}{(R_m^2 - R_r^2)} \cdot \sin^2\left(vp_s \frac{\alpha_p}{2}\right) \right] \tag{27}$$

$$H_v = \left(\frac{R_m}{R_s}\right)^{vp_s} \frac{R_s R_m^2}{(vp_s+2)} \left[1 - \left(\frac{R_r}{R_m}\right)^{vp_s+2}\right] + \left(\frac{R_r}{R_s}\right)^{vp_s} R_s R_r^2 E_v \tag{28}$$

$$E_v = \begin{cases} \frac{\left(\frac{R_m}{R_r}\right)^{-vp_s+2} - 1}{(-vp_s+2)} & \text{for } vp \neq 2 \\ \ln\left(\frac{R_m}{R_r}\right) & \text{for } vp = 2 \end{cases} \tag{29}$$

V. COMPARISON WITH FINITE-ELEMENT PREDICTIONS AND INVESTIGATION

The developed analytical model has been applied to the three three-phase, 12-slot/10-pole motors whose parameters are given in Table I, and the calculated magnet eddy-current loss has been compared with predictions from 2-D time-stepped FEA, using the *MEGA* software package. Fig. 5 shows the variation of the magnet loss at rated current, viz. 10 A peak, for BLAC operation. As will be seen, good agreement is achieved. As shown in Tables II–IV, the magnet loss that results in Motor III is approximately three times higher than that for Motor I, while the loss that results in Motor II is approximately double that for Motor I.

TABLE III
ALTERNATE TEETH WOUND—EDDY-CURRENT LOSS, BLAC MODE

Space harmonic v	Loss in all magnets (W/m)			
	400rpm	800rpm	1200rpm	1600rpm
1	1.62	6.47	14.57	25.9
5	0	0	0	0
7	1.23	4.93	11.09	19.71
11	0.02	0.071	0.160	0.28
13	0.007	0.030	0.067	0.119
17	0.01	0.043	0.097	0.173
19	0.05	0.022	0.454	0.806
Total	2.94	11.57	26.43	46.99

TABLE IV
ALTERNATE TEETH WOUND ON WIDER TEETH—EDDY-CURRENT LOSS, BLAC MODE

Space harmonic v	Loss in all magnets (W/m)			
	400rpm	800rpm	1200rpm	1600rpm
1	2.84	11.37	25.58	45.47
5	0	0	0	0
7	0.90	3.56	8.10	14.39
11	0.002	0.007	0.015	0.027
13	0.10	0.40	0.90	1.61
17	0.02	0.084	0.19	0.34
19	0.016	0.062	0.14	0.25
Total	3.88	15.52	34.92	62.08

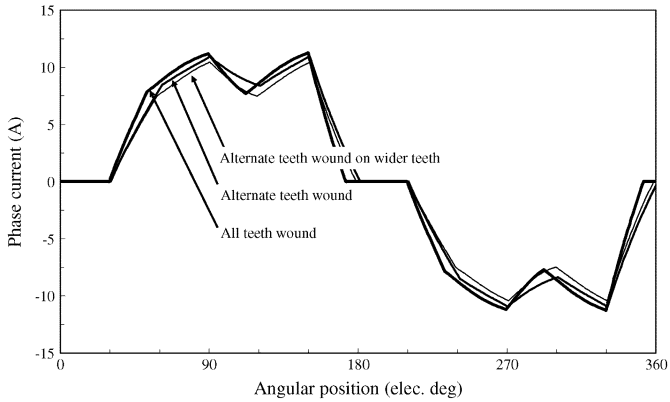

Fig. 6. Simulated BLDC phase current waveforms.

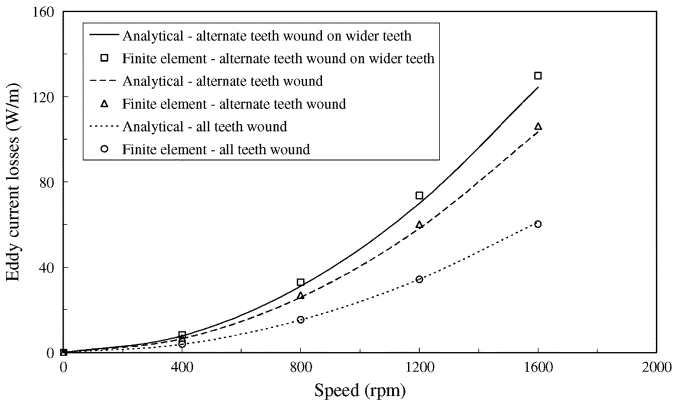

Fig. 7. Variation of eddy-current loss with rotor speed, BLDC mode. (a) All teeth wound. (b) Alternate teeth wound. (c) Alternate teeth wound on wider teeth.

The developed analytical model has also been used to predict the magnet loss when the motors are operated in BLDC mode

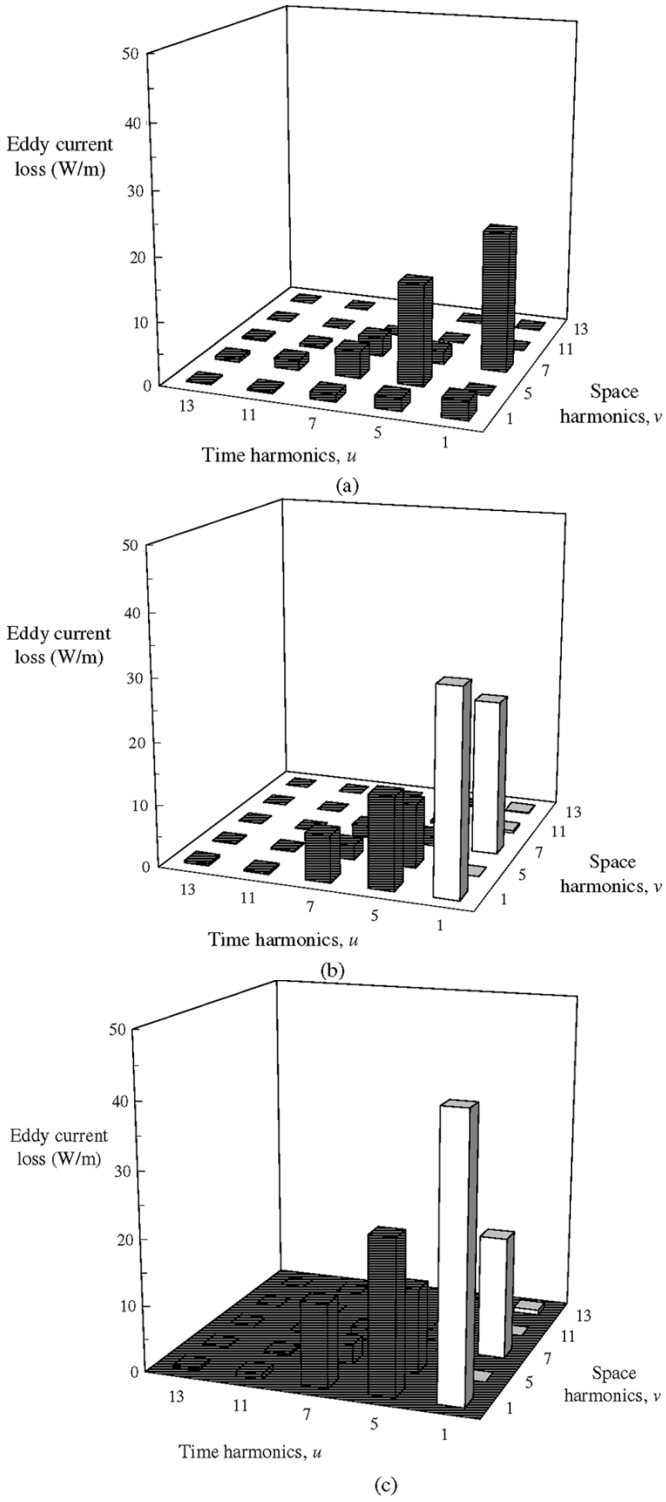

Fig. 8. Loss spectra at 1600 rpm, BLDC mode. (a) All teeth wound. (b) Alternate teeth wound. (c) Alternate teeth wound on wider teeth.

at rated current, using the phase current waveforms shown in Fig. 6 deduced from dynamic simulations. The slight difference in the waveforms is due to the different winding self and mutual inductances [4], these being 2.91 and −0.32 mH, 4.62 mH and −0.01mH, and 4.85 mH and −0.001 mH, respectively, for motors I, II, and III. Again, good agreement is obtained between the analytical and finite-element calculated eddy-current loss as will be evident from Fig. 7. In addition, it will be seen that the magnet

TABLE V
MAGNET EDDY-CURRENT LOSS FOR DIFFERENT STATOR CURRENT DENSITIES

Current density, A/mm^2 (Current, A)	6.1 (9.35)	15 (23)	30 (46)
Loss, W	400rpm/1600rpm		
Motor I - all teeth wound	0.066/1.05	0.4/6.37	1.6/25.5
Motor II- alternate teeth wound	0.15/2.35	0.9/14.2	3.59/56.9
Motor III - alternate teeth wound on wider teeth	0.19/3.1	1.19/18.8	4.74/75.1

loss in Motor II is approximately twice that in Motor I, and that BLDC operation results in a significantly higher eddy-current loss than BLAC operation. Since the electromagnetic torque is produced by the fifth space-harmonic MMF, which rotates in synchronism with the rotor, the magnet loss is zero for the combination of this space harmonic and the fundamental time harmonic for all three motors. When all the teeth are wound [Fig. 8(a)], the magnet loss associated with the fundamental component of the phase current is very small, the majority of the loss being due to the seventh space-harmonic MMF and the fifth and seventh current time harmonics. In contrast, when alternate teeth are wound, the loss is due mainly to the fundamental and seventh space-harmonic MMFs and the fundamental, fifth, and seventh current time harmonics [Fig. 8(b) and (c)].

The eddy-current loss is influenced significantly by the maximum current density, or electric loading. By way of example, Table V compares the eddy-current loss that results when the three motors are operated in BLAC mode at current densities of 6, 15, and 30 A/mm^2, which correspond approximately to natural air-cooling, forced air-cooling, and water cooling, respectively. As can be seen, the loss varies approximately in proportion to the square of the current density and rotor speed.

VI. CONCLUSION

An analytical model for predicting the eddy-current loss in the surface-mounted permanent magnets of a brushless machine due to the armature reaction field has been presented. The method has been validated by FEA and used to compare the loss that results when all the teeth are wound and alternate teeth are wound. It has been shown that BLDC operation results in a significantly higher magnet loss than BLAC operation, that the loss that results when alternate teeth are wound is almost double that when all the teeth are wound, and that the use of unequal tooth widths results in the highest eddy-current loss.

REFERENCES

[1] J. R. Hendershot Jr. and T. J. E. Miller, *Design of Brushless Permanent Magnet Motors*. Oxford, U.K.: Magna Physics, 1994.

[2] R. Mizutani and N. Matsui, "Optimum design approach for low-speed, high-torque permanent magnet motors," *Trans. Elect. Eng. Jpn.*, vol. 135, no. 4, pp. 52–63, 2001.

[3] J. Cros and P. Viarouge, "Synthesis of high performance PM machines with concentrated windings," *IEEE Trans. Energy Convers.*, vol. 17, no. 2, pp. 248–253, Jun. 2002.

[4] D. Ishak, Z. Q. Zhu, and D. Howe, "Permanent magnet brushless machines with unequal tooth widths and similar slot and pole numbers," *IEEE Trans. Ind. Appl.*, vol. 41, no. 2, pp. 584–590, Mar.–Apr. 2005.

[5] C. C. Chan, J. Z. Jiang, G. H. Chen, X. Y. Wang, and K. T. Chau, "A novel polyphase multipole square-wave permanent magnet motor drive for electric vehicles," *IEEE Trans. Ind. Appl.*, vol. 30, no. 5, pp. 1258–1266, Sep.–Oct. 1994.

[6] A. G. Jack, B. C. Mecrow, and J. A. Haylock, "A comparative study of permanent magnet and switched reluctance motors for high-performance fault-tolerant applications," *IEEE Trans. Ind. Appl.*, vol. 32, no. 4, pp. 889–895, Jul.–Aug. 1996.

[7] K. Atallah, D. Howe, P. H. Mellor, and D. A. Stone, "Rotor loss in permanent magnet brushless AC machines," *IEEE Trans. Ind. Appl.*, vol. 36, no. 6, pp. 1612–1618, Nov.–Dec. 2000.

[8] Z. Q. Zhu, K. Ng, N. Schofield, and D. Howe, "Improved analytical modeling of rotor eddy current loss in brushless machines equipped with surface-mounted permanent magnets," *Proc. Inst. Elect. Eng.—Elect. Power Appl.*, vol. 151, no. 6, pp. 641–650, 2004.

[9] F. Deng, "Commutation caused eddy current losses in permanent magnet brushless DC motors," *IEEE Trans. Magn.*, vol. 33, no. 5, pp. 4310–4318, Sep. 1997.

[10] ——, "Analytical modeling of eddy current losses caused by pulse-width-modulation switching in permanent-magnet brushless DC motors," *IEEE Trans. Magn.*, vol. 34, no. 5, pp. 3728–3726, Sep. 1998.

[11] Z. Q. Zhu, K. Ng, N. Schofield, and D. Howe, "Analytical prediction of rotor eddy current losses in brushless motors with surface-mounted permanent magnets, part I: Based on magnetostatic field distribution model," in *Proc. Int. Conf. Electrical Machines & Systems*, Shenyang, China, Aug. 18–20, 2001, pp. 806–809.

[12] Z. Q. Zhu and D. Howe, "Instantaneous magnetic field distribution in brushless permanent magnet dc motors, part III: Effect of stator slotting," *IEEE Trans. Magn.*, vol. 29, no. 1, pp. 143–151, Jan. 1993.

Manuscript received April 9, 2005; revised June 7, 2005.

Dahaman Ishak received the B.Eng. degree from the University of Syracuse, Syracuse, NY, in 1990 and the M.Sc. degree from University of Newcastle upon Tyne, Newcastle, U.K., in 2001, both in electrical engineering. He is currently a Ph.D. student in the Department of Electronic and Electrical Engineering, University of Sheffield, Sheffield, U.K., working on the design and analysis of low-speed, high-torque permanent-magnet brushless machines.

Z. Q. Zhu (M'90–SM'00) received the B.Eng. and M.Sc. degrees from Zhejiang University, Hangzhou, China, in 1982 and 1984, respectively, and the Ph.D. degree from the University of Sheffield, Sheffield, U.K., in 1991, all in electrical engineering.

From 1984 to 1988, he lectured in the Department of Electrical Engineering at Zhejiang University. In 1988, he joined the University of Sheffield, where since 2000 he has been a Professor of Electrical Engineering. His current major research interests include the application, control, and design of permanent-magnet machines and drives.

David Howe received the B.Tech. and M.Sc. degrees from the University of Bradford, Bradford, U.K., in 1966 and 1967, respectively, and the Ph.D. degree from the University of Southampton, Southampton, U.K., in 1974, all in electrical power engineering.

He has held academic posts at Brunel and Southampton Universities, and spent a period in industry with NEI Parsons Ltd. working on electromagnetic problems related to turbogenerators. He is currently a Professor of Electrical Engineering at the University of Sheffield, Sheffield, U.K., where he heads the Electrical Machines and Drives Research Group. His research activities span all facets of controlled electrical drive systems, with particular emphasis on permanent-magnet excited machines.

Prof. Howe is a Chartered Engineer, a Fellow of the Royal Academy of Engineering, and a Fellow of the Institution of Electrical Engineers, U.K.